SPECT Image Analysis Using Statistical Parametric Mapping in Patients with Parkinson's Disease

Yukari Imon, Hiroshi Matsuda, Masafumi Ogawa, Daiji Kogure and Nobuhiko Sunohara

Departments of Radiology and Neurology, National Center Hospital for Mental, Nervous and Muscular Disorders, National Center of Neurology and Psychiatry, Tokyo, Japan

This study investigated alterations in regional cerebral blood flow (rCBF) in patients with Parkinson's disease using statistical parametric mapping (SPM). **Methods:** Noninvasive rCBF measurements using ^{99m}Tc-ethyl cysteinate dimer (ECD) SPECT were performed on 28 patients with Parkinson's disease and 48 age-matched healthy volunteers. The Parkinson's disease patients were divided into two groups, 16 patients with Hoehn and Yahr stage I or II and 12 patients with Hoehn and Yahr stage III or IV. We used the raw data (absolute rCBF parametric maps) and the adjusted rCBF images in relative flow distribution (normalization of global CBF for each subject to 50 mL/100 g/min with proportional scaling) to compare these groups with SPM. **Results:** In patients with stage I or II Parkinson's disease, we found a diffuse decrease in absolute rCBF in the whole brain with sparing of the central gray matter, hippocampus and right lower temporal lobe compared with healthy volunteers. Adjusted rCBF increased in both putamina and the right hippocampus. In patients with stage III or IV disease, rCBF decreased throughout the whole brain. Adjusted rCBF increased bilaterally in the putamina, globi pallidi, hippocampi and cerebellar hemispheres (dentate nuclei) and in the left ventrolateral thalamus, right insula and right inferior temporal gyrus. **Conclusion:** SPM analysis showed that significant rCBF changes in Parkinson's disease accompanied disease progression and related to disease pathophysiology in the functional architecture of thalamocortex-basal ganglia circuits and related systems.

Key Words: SPECT; regional cerebral blood flow; Parkinson's disease; statistical parametric mapping

J Nucl Med 1999; 40:1583–1589

Because Parkinson's disease results from degeneration of dopaminergic nigrostriatal neurons (*1*), one would expect that dopamine depletion within basal ganglia might result in consistent alterations of local functional activity and, consequently, rates of regional cerebral metabolism (rCMR) or regional cerebral blood flow (rCBF). However, rCMR or rCBF in the basal ganglia of Parkinson's disease patients has been reported to be reduced (*2*), increased (*3–5*) or unchanged (*6–8*) from control values. In addition, diffuse or focal cortical abnormalities have been reported (*7,9–11*), but the results have not been consistent.

This inconsistency may have several causes. First, most investigators analyzed absolute rCBF or rCMR values, which are susceptible to general arousal, aging, drug effects, and so on. Second, some studies used two-dimensional techniques or older PET scanners with low resolution and few tomographic planes. Third, selected regions of interest (ROIs) were studied with a priori hypotheses. This approach, although generally accepted, is limited in that the sample selected depends on the observer's a priori choice and hypothesis. Large areas of the brain are left unexplored. An alternative approach is voxel-by-voxel analysis in the stereotactic space to avoid subjectivity and to adopt the principle of data-driven analysis. Such an approach is well established in the field of functional neuroimaging analysis. A software package known as statistical parametric mapping (SPM) has been developed that not only spatially normalizes PET or SPECT images to a standardized stereotactic space but also can then perform statistical analyses on groups of images (*12,13*). We applied this technique to SPECT to clarify the pathogenesis of Parkinson's disease by searching for rCBF alterations in the entire brain. The applicability of SPM to Parkinson's disease was recently validated in PET studies using $H_2{}^{15}O$ or ^{18}F-fluorodeoxyglucose (FDG) (*14,15*).

MATERIALS AND METHODS

Subjects

We studied 28 Parkinson's disease patients (10 men, 18 women; mean age 63.5 y; range 38–79 y). Idiopathic Parkinson's disease was diagnosed if a patient had resting tremor, cogwheel rigidity and bradykinesia. Patients with a history of known causes such as encephalitis or neuroleptic treatment were excluded. The Parkinson's disease patients did not have a supranuclear gaze abnormality, myoclonus, autonomic dysfunction, apraxia, ataxia, dementia or a convincing response to levodopa. They were staged using the method of Hoehn and Yahr (*16*). Eight patients had disease in stage

Received Jul. 29, 1998; revision accepted Mar. 26, 1999.

For correspondence or reprints contact: Hiroshi Matsuda, MD, Department of Radiology, National Center Hospital for Mental, Nervous and Muscular Disorders, NCNP, 4-1-1, Ogawahigashi, Kodaira, Tokyo 187-8551, Japan.

TABLE 1
Subjects Studied

Characteristic	Healthy volunteers (n = 48)	Patients with Parkinson's disease (n = 28)	
		Hoehn and Yahr I or II (n = 16)	Hoehn and Yahr III or IV (n = 12)
Age (y)*	58.4 ± 10.0	63.6 ± 9.9	63.3 ± 5.9
Sex (M/F)	22/26	5/11	5/7
Symptom duration (y)*	NA	6.1 ± 6.3	11.0 ± 5.9
Predominantly symptomatic body side (right/left/both)	NA	8/8/0	7/3/2

*Mean ± SD.
NA = not applicable.

I, 8 in stage II, 9 in stage III and 3 in stage IV. Patients with stage I or II disease were classed as one group, and patients with stage III or IV disease were classed as a second group. The patients were medicated with various combinations of L-dopa with a decarboxylase inhibitor (carbidopa or benserazide), anticholinergic agents, amantadine hydrochloride and dopamine (D_2)-receptor agonist. Except for L-dopa, no significant differences in dose of drugs were seen between the first group and the second group.

Forty-eight control subjects (22 men, 26 women; mean age 58.4 y; range 38–79 y) were also studied. They were healthy volunteers who had no neurologic or psychiatric disorders, including alcoholism, substance abuse, atypical headache, head trauma with consciousness loss and asymptomatic cerebral infarction detected by T2-weighted MRI. The portion of the study involving healthy volunteers was approved by the ethics committee of the National Center of Neurology and Psychiatry. All healthy volunteers gave informed consent. Tables 1 and 2 summarize the subject profiles.

Global and Regional Cerebral Blood Flow Measurements

Before undergoing SPECT, all subjects received an intravenous line while lying down with eyes closed. Each subject received a 600-MBq intravenous injection of ^{99m}Tc-ethyl cysteinate dimer (ECD). The global CBF was noninvasively measured using graphic analysis as described previously (*17,18*), without blood sampling.

TABLE 2
Chronic Oral Antiparkinsonian Drug Therapy

Drug	Hoehn and Yahr I or II (n = 16)		Hoehn and Yahr III or IV (n = 12)	
	No.	Dose (mg/d)	No.	Dose (mg/d)
Trihexyphenidyl*	10	4.6 ± 1.3	4	5.7 ± 0.8
L-dopa*	8	244 ± 73	12	354 ± 134
Amantadine*	3	216 ± 76	6	208 ± 49
Bromocriptine	1	15	3	15
Pergolide*	6	0.3 ± 0.4	2	0.6 ± 0.5
Talipexole	0	0	2	0.8

*Mean ± SD.

The passage of tracer from the aortic arch to the brain was monitored in a 128 × 128 format for 100 s at 1-s intervals using a rectangular gamma camera with the parallel-hole collimator of the three-head SPECT system (Multispect3; Siemens Medical Systems, Hoffman Estates, IL). ROIs were hand-drawn over the aortic arch (ROI_{aorta}) and both brain hemispheres (ROI_{brain}). A hemispheric brain perfusion index (BPI) (*17*) was determined before the start of the initial backdiffusion of tracer from brain to blood as follows:

$$BPI = 100 \times ku \frac{10 \times ROI_{aorta}\ size}{ROI_{brain}\ size}, \quad \text{Eq. 1}$$

where ku is the unidirectional influx rate for the tracer from blood to brain, determined by the slope of the line in graphic analysis within the first 30 s after injection. Then, BPI (x) was converted to global CBF values (y) obtained by ^{133}Xe inhalation SPECT studies ($y = 2.60x + 19.8$) (*17*).

Ten minutes after the injection of ^{99m}Tc-ECD, brain SPECT was performed using a system equipped with high-resolution fanbeam collimators. For each camera, the projection data were obtained in a 128 × 128 format for 24 angles in 120° increments at a rate of 50 s per angle. A Shepp and Logan Hanning filter was used for SPECT image reconstruction at 0.75 cycle/cm (*19*). Attenuation correction was performed using Chang's method (*20*). To calculate rCBF and to correct for incomplete retention of ^{99m}Tc-ECD in the brain, the following linearization algorithm (*21*) of a curve-linear relationship between brain activity and blood flow was applied:

$$Fi = Fr \times \frac{a \times (Ci/Cr)}{[1 + a - (Ci/Cr)]}, \quad \text{Eq. 2}$$

where Fi and Fr represent CBF values for a region i and a reference region, respectively, and Ci and Cr are the SPECT counts for the region i and the reference region, respectively. The cerebral hemisphere was used as the reference region, and global CBF obtained from graphic analysis was substituted for Fr. The linearization factor α was set to 2.59, which was a proposed value by Friberg et al. (*21*).

Image Formatting

All subsequent image manipulation and data analysis were performed on a personal computer using a UNIX operating system (Linux, version 4.2; Red Hat Software, Inc., Research Triangle Park, NC). The software for image manipulation included Matlab, version 4.2c (Mathworks, Inc., Natick, MA) and SPM (*12,13*). The image volumes of transverse slices were made compatible with SPM by creation of usable headers for the images. For each image, a file was created that contained data on image size, number of slices, pixel depth (16-bit), maximum pixel value and voxel size. All slices of a brain image were then sampled and averaged to arrive at a mean pixel intensity for that image. The intensity threshold was set at 80% of the whole-brain mean. This level eliminated low-intensity background noise inherent in the images and effectively removed brain-edge halo caused by partial-volume error, without losing any image data specific to the brain. The images were then spatially normalized in SPM to a standardized stereotactic space based on the Talairach and Tournoux atlas (*22*), using 12-parameter linear affine normalization and a further eight nonlinear iteration algorithms. The normalization routine also included further isotropic smoothing, to a total of 12 mm. This smoothing corresponds to almost two times the resolution (7.6 mm

full width at half maximum) of the SPECT scanner. The initial image parameters were 128 × 128 × n, in which n is the number of slices (varied from 50 to 70). The final image format was 16-bit, with a size of 79 × 95 × 68 and a voxel size of 2 × 2 × 2 mm.

Image Analysis

Data were analyzed using SPM. Statistical parametric maps are spatially extended statistical processes and were used to characterize regionally specific effects in imaging data. SPM combines the general linear model (to create the statistical map, or SPM) and the theory of Gaussian fields to make statistical inferences about regional effects (*23,24*). To examine images for specific regions showing differences in perfusion between the Parkinson's disease patients and the healthy volunteers, two comparisons were performed. The first examined areas of increased perfusion—and the second, areas of decreased perfusion—in the Parkinson's disease group compared with the healthy control group. The analysis was performed with and without use of global CBF changes between SPECT images as a confounding covariate. We first used the raw data (absolute rCBF parametric maps) and then adjusted rCBF images (normalization of global CBF for each subject to 50 mL/100 g/min with proportional scaling) to compare the relative rCBF distribution in the two groups. The resulting set of values for each comparison constituted a statistical parametric map of the t statistic SPM{t}.The SPM{t}maps were then transformed to the unit of normal distribution, (SPM{Z}), and reached a threshold at $P = 0.001$. The resulting regions were then examined in terms of size and peak height. The significance of each region was estimated at a threshold of $P = 0.05$ using distributional approximations from the theory of Gaussian fields (*23*). These areas of significance were best seen when overlaid on a normalized MR image to obtain a clear view of the location of the perfusion changes.

RESULTS

Global Effects

The global CBF of Parkinson's disease patients—35.9 ± 4.9 mL/100 g/min (stages I and II 37.5 ± 4.9 mL/100 g/min, stages III and IV 33.9 ± 4.3 mL/100 g/min)—was significantly lower than that of healthy volunteers (42.0 ± 3.8 mL/100 g/min) (Tukey-Kramer $P < 0.001$).

Regional Effects

Absolute rCBF. Figure 1 shows the voxels with a significant decline in absolute rCBF in Parkinson's disease patients compared with healthy volunteers (in no voxel did rCBF significantly increase). A significant rCBF reduction was observed in the whole brain of Parkinson's disease patients in stages III and IV. In patients with stage I or II disease, all

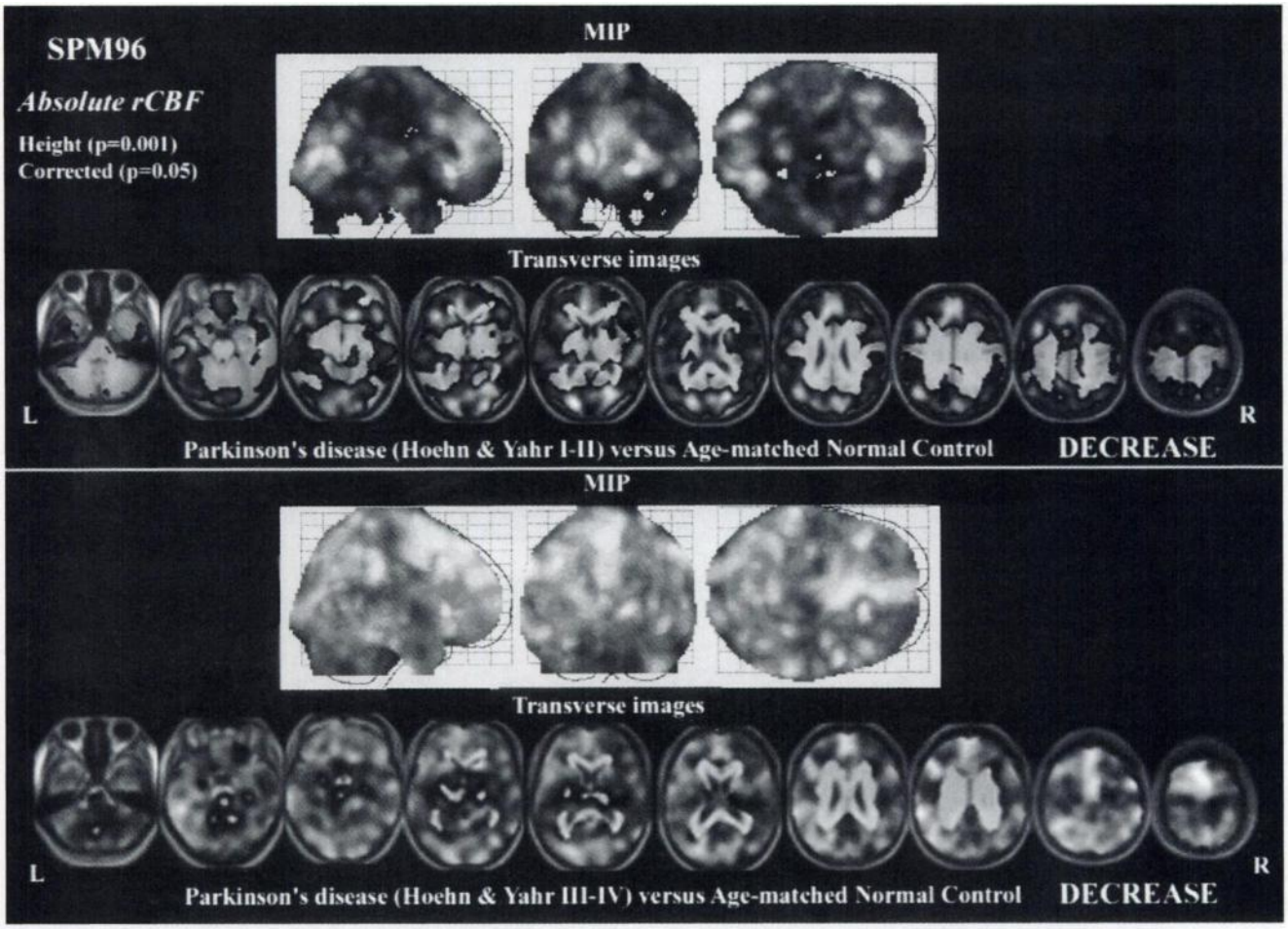

FIGURE 1. Absolute regional cerebral blood flow (rCBF) decrease shown by statistical parametric mapping (SPM) in patients with Parkinson's disease compared with healthy volunteers. Significant decrease is shown as maximum intensity projection (MIP) and gray-scale areas superimposed on transverse slices of standard MR images.

TABLE 3
Location and Peaks of Significant ($P < 0.001$) Decrease in Absolute Regional Cerebral Blood Flow in Patients with Parkinson's Disease Compared with Healthy Volunteers

Stage	Structure	Coordinates			*z* score
		x	y	z	
Hoehn and Yahr I or II	Left primary visual cortex	−22	−84	12	5.15
	Right primary visual cortex	24	−74	14	5.10
		22	−92	2	4.91
	Left medial frontal gyrus	−8	36	20	4.92
	Left anterior cingulate gyrus	−8	36	8	4.90
Hoehn and Yahr III or IV	Left inferior parietal lobe	−66	−36	36	6.38
	Left superior frontal gyrus	−6	14	58	6.19
	Right superior frontal gyrus	2	6	62	6.15
		4	36	54	6.04
		6	−2	72	6.01
	Right middle frontal gyrus	58	0	48	6.03

cerebral cortical regions except the right lower temporal cortex showed a significant reduction, whereas basal ganglia, thalami, brain stems, hippocampi and cerebellums showed no significant reduction. Table 3 lists the peaks of the most significant declines in absolute rCBF obtained in this analysis with the x, y and z coordinates of Talairach and Tournoux (*22*), in millimeters, as well as the corresponding *z* scores.

Adjusted rCBF. Figure 2 and Table 4 show the voxels with a significant increase in adjusted rCBF in Parkinson's disease patients compared with healthy volunteers (no voxel significantly decreased). In patients with stage I or II disease, the adjusted rCBF significantly increased in both putamina and the right hippocampus compared with healthy volunteers. In patients with stage III and IV disease, adjusted

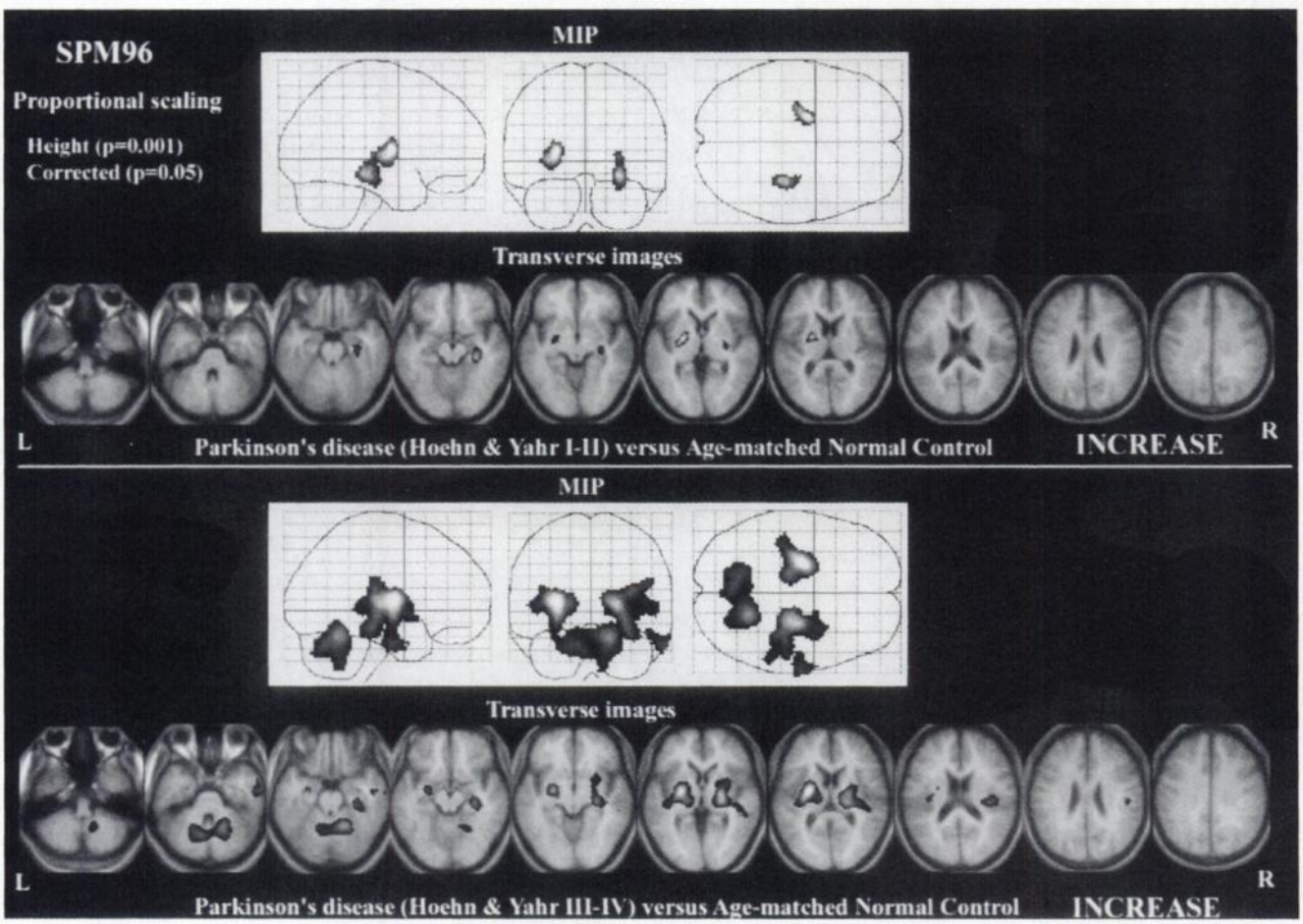

FIGURE 2. Adjusted regional cerebral blood flow (rCBF) increase shown by statistical parametric mapping (SPM) in patients with Parkinson's disease compared with healthy volunteers. MIP = maximum intensity projection.

TABLE 4
Location and Peaks of Significant ($P < 0.001$) Increase in Adjusted Regional Cerebral Blood Flow in Patients with Parkinson's Disease Compared with Healthy Volunteers

Stage	Structure	Coordinates			z score
		x	y	z	
Hoehn and Yahr I or II	Left putamen	−24	−6	4	4.59
	Right hippocampus	30	−22	−12	4.24
	Right putamen	30	−18	2	3.73
Hoehn and Yahr III or IV	Left putamen	−26	−8	8	6.61
		−30	−16	10	5.56
	Left globus pallidus	−26	−8	−6	5.26
	Left thalamus (ventrolateralis)	−18	−18	4	4.78
	Left hippocampus	−26	−8	−20	3.63
	Right globus pallidus	24	−12	6	5.94
		28	2	−2	4.03
	Right putamen	30	−18	−6	4.85
	Right hippocampus	32	−24	−16	4.84
	Right insula	36	−22	16	4.64
		50	−20	22	4.09
	Right dentate nucleus	18	−54	−22	5.22
		14	−54	−38	4.04
	Left dentate nucleus	−10	−62	−28	4.50
		−8	−50	−16	3.41
	Right inferior temporal gyrus	64	−8	−32	4.39
		52	−12	−20	3.52

rCBF increased in both putamina, globi pallidi, hippocampi and cerebellar hemispheres (dentate nuclei), the left thalamus (nucleus ventrolateralis), the right insula and the right inferior temporal gyrus compared with healthy volunteers.

DISCUSSION

Global CBF and CMR in Parkinson's disease patients have been reported to be uniformly lower than (*4,7,25*) or the same as (*11*) those in healthy volunteers. For oxygen, global CBF was reported to be lower than global CMR (*4*) in patients with advanced Parkinson's disease. This uncoupling of CBF and CMR may be due to vasoconstriction from loss of dopaminergic innervation of blood vessels in patients with advanced Parkinson's disease (*4*). In this study, a global CBF decrease of 11% and 20% was observed in patients with stage I and II disease and stage III and IV disease, respectively. This reduction agreed well with that previously reported (*4,7,25*).

Many investigators have reported changes in basal ganglion rCBF in patients with Parkinson's disease, but the results have been somewhat contradictory. Asymmetry of rCBF and rCMR in basal ganglia has sometimes been reported (*2,5,11*). Although an increase in the globus pallidus contralateral to the most affected extremities was frequently found, Perlmutter and Raichle (*11*) reported pallidal rCBF asymmetry unrelated to the side of motor impairment.

Several groups have also examined the effects of L-dopa on rCBF and rCMR in patients with Parkinson's disease. Some groups used PET to examine the effects of oral therapy maintained for at least 2 wk and found no difference between Parkinson's disease patients and healthy volunteers (*26,27*). Miletich et al. (*5*) reported that chronic oral therapy attenuated increased rCBF in the basal ganglia contralateral to the affected body side. Pallidal rCBF asymmetry was reported to decrease after L-dopa therapy in hemiparkinsonism (*11*). With two-dimensional ^{133}Xe techniques, either no change (*25*) or increased perfusion (*28*) has been reported for the cerebral cortex.

This study showed a significant increase in adjusted rCBF in basal ganglia, ventrolateral thalami, hippocampi, insulae, inferior temporal gyri and cerebellar dentate nuclei, with little asymmetry and with greater prominence in patients with severe Parkinson's disease. The relationship between rCBF changes and the affected body side should be further investigated using more patients with hemiparkinsonism. Moreover, we cannot exclude the influence of drug therapy on these rCBF distribution findings. Patients with stage III or IV disease received more L-dopa than did patients with stage I or II disease. However, taking into account the previously reported (*5,11*) attenuation of rCBF in basal ganglia after L-dopa therapy, we believe these rCBF changes in basal ganglia may relate to the pathophysiology of Parkinson's disease and may correlate with its progression.

Although the mechanism for the increase in adjusted rCBF changes in these structures is difficult to explain clearly, these structures are part of the complicated functional architecture of thalamocortex-basal ganglion circuits (*29,30*). Our results support the effectiveness of stereoencephalotomy in the treatment of Parkinson's disease. Pallidotomy (*31,32*) or ventrolateral thalamotomy (*33*) has been performed for amelioration of rigidity or tremor and other

parkinsonian symptoms. This amelioration may be explained by a release of GABAergic suppression and an acceleration of neuronal discharge in the globus pallidus because of decreased dopamine in the striatum (*34*). A PET study using ^{18}F-FDG suggested that pallidotomy reduced the preoperative overaction of the pallidothalamic projection (*15*). Pallidotomy and ventrolateral thalamotomy were assumed to isolate the projection and improve the rigidity. The basal ganglion recipient zones within the ventrolateral thalamus receive ascending, convergent input from the cerebellum and return their own projections exclusively to the primary motor cortex (*30*). The adjusted rCBF increase in cerebellar dentate nuclei that we found may result from compensation for movement disturbances such as postural instability in advanced stages of disease through this cerebellar efferent projection to the ventrolateral thalamus. The reason for elevations of adjusted rCBF in the hippocampus remains unclear. The basal ganglia have been reported to be capable of participating concurrently in the limbic process (*29*). This limbic circuit might be involved in certain pathologic conditions with significant behavioral manifestations (*30*).

Previous functional studies of Parkinson's disease using an ROI technique have not observed rCBF and rCMR changes in ventrolateral thalami, cerebellar dentate nuclei, and hippocampi as shown in this study. A new technique, SPM, allowed us to handle images and analyze data reliably and objectively and makes possible the complicated analyses that could improve interstudy variability caused by the analytic process itself.

In recent years, dopamine (D_2)-receptor and dopamine-transporter imaging has become available for examining patients with Parkinson's disease and has improved its diagnosis remarkably (*35–37*). However, ^{99m}Tc-ECD is widespread and easily available in any institution with SPECT, and this study shows the usefulness of combining ^{99m}Tc-ECD SPECT with SPM for examinating Parkinson's disease patients.

CONCLUSION

This SPECT study using an SPM technique shows significant rCBF changes in Parkinson's disease patients compared with age-matched healthy volunteers. As the stage of disease advanced, adjusted rCBF increased in thalamocortex-basal ganglia circuits and in related cerebellar efferent and limbic systems. The SPM technique is useful for objective investigation of rCBF alterations in Parkinson's disease patients.

REFERENCES

1. Hornykiewicz O. Dopamine (3-hydroxytyramine) and brain function. *Pharmacol Rev.* 1966;18:925–964.
2. Henriksen L, Boas J. Regional cerebral blood flow in hemiparkinsonian patients: emission computerized tomography of inhaled ^{133}xenon before and after levodopa. *Acta Neurol Scand.* 1985;71:257–266.
3. Martin WRW, Beckman JH, Calne DB, et al. Cerebral glucose metabolism in Parkinson's disease. *Can J Neurol Sci.* 1984;11:169–173.
4. Wolfson LI, Leenders KL, Brown LL, Jones T. Alterations of cerebral blood flow and oxygen metabolism in Parkinson's disease. *Neurology.* 1985;35:1399–1405.
5. Miletich RS, Quarantelli M, Chiro G. Regional cerebral blood flow imaging with ^{99m}Tc-bicisate SPECT in asymmetric Parkinson's disease: studies with and without chronic drug therapy. *J Cereb Blood Flow Metab.* 1994;14(suppl 1):S106–S114.
6. Rougemont D, Baron JC, Collard P, Bustany P, Comar D, Agid Y. Local cerebral metabolic rate of glucose (lCMRglc) in treated and untreated patients with Parkinson's disease. *J Cereb Blood Flow Metab.* 1983;3(suppl 1);S504–S505.
7. Kuhl DE, Metter EJ, Reige WH. Patterns of local cerebral glucose utilization determined in Parkinson's disease by the (^{18}F)fluorodeoxyglucose method. *Ann Neurol.* 1984;15:419–424.
8. Pizzolato G, Dam M, Borsato N, et al. [^{99m}Tc]-HM-PAO SPECT in Parkinson's disease. *J Cereb Blood Flow Metab.* 1988;8(suppl 1):S101–S108.
9. Lenzi GL, Jones T, Reid GL, Moss S. Regional impairment of cerebral oxydative metabolism in Parkinson's disease. *J Neurol Nerosurg Psychiatry.* 1979;22:59–62.
10. Globus M, Mildworf B, Melamed E. Cerebral blood flow and cognitive impairment in Parkinson's disease. *Neurology.* 1985;35:1135–1139.
11. Perlmutter JS, Raichle ME. Regional blood flow in hemiparkinsonism. *Neurology.* 1985;35:1127–1134.
12. Friston KJ, Ashburner J, Poline JB, Frith CD, Heather JD, Frakowiak RSJ. Spatial realignment and normalization of images. *Hum Brain Mapping.* 1995;2:165–189.
13. Friston KJ, Holmes AP, Worsley KJ, Poline JB, Frith CD, Frackowiak RSJ. Statistical parametric maps in functional imaging: a general approach. *Hum Brain Mapping.* 1995;2:189–210.
14. Samuel M, Ceballos-Baumann AO, Turjansk N, et al. Pallidotomy in Parkinson's disease increases supplementary motor area and prefrontal activation during performance of volitional movements: an $H_2{}^{15}O$ PET study. *Brain.* 1997;120:1301–1313.
15. Eidelberg D, Moeller JR, Ishikawa T, et al. Regional metabolic correlates of surgical outcome following unilateral pallidotomy for Parkinson's disease. *Ann Neurol.* 1996;39:450–459.
16. Hoehn MM, Yahr MD. Parkinsonism: onset, progression and mortality. *Neurology.* 1967;17:427–442.
17. Matsuda H, Yagishita A, Tsuji S, Hisada K. A quantitative approach to technetium-99m ethyl cysteinate dimer: a comparison with technetium-99m hexamethylpropylene amine oxime. *Eur J Nucl Med.* 1995;22:633–637.
18. Takeuchi R, Matsuda H, Yonekura Y, Sakahara H, Konishi J. Noninvasive quantitative measurements of regional cerebral blood flow using technetium-99m-L,L-ECD SPECT activated with acetazolamide: quantification analysis by equal-volume-split ^{99m}Tc-ECD consecutive SPECT method. *J Cereb Blood Flow Metab.* 1997;17:1020–1032.
19. Shepp LA, Logan BF. The Fourier reconstruction of a head section. *IEEE Trans Nucl Sci.* 1974;21:12–43.
20. Chang LT. A method for attenuation correction in radionuclide computed tomography. *IEEE Trans Nucl Sci.* 1978;25:638–643.
21. Friberg L, Andersen AR, Lassen NA, Holm S, Dam M. Retention of ^{99m}Tc-bicisate in the human brain after intracarotid injection. *J Cereb Blood Flow Metabol.* 1994;14(suppl 1):S19–S27.
22. Talairach J, Tournoux P. *Co-planar Sterotactic Atlas of the Human Brain.* Stuttgart, Germany: Thieme; 1988.
23. Friston KJ, Worsley KJ, Frackowiak RSJ, Mazziotta JC, Evans AC. Assessing the significance of focal activations using their spatial extent. *Hum Brain Mapping.* 1994;1:214–220.
24. Friston KJ, Frith CD, Liddle PF, Frackowiak RSJ. Comparing functional (PET) images: the assessment of significant change. *J Cereb Blood Flow Metab.* 1991;11:690–699.
25. Melamed E, Lavy S, Cooper G, Bentin S. Regional cerebral blood flow in parkinsonism: measurement before and after levodopa. *J Neurol Sci.* 1978;38:391–397.
26. Leenders KL, Wolfson L, Gibbs JM, Wise RJS, Causon R, Jones T, Legg NJ. The effects of L-dopa on regional cerebral blood flow and oxygen metabolism in patients with Parkinson's disease. *Brain.* 1985;108:171–191.
27. Otsuka M, Ichiya Y, Hosokawa S, et al. Striatal blood flow, glucose metabolism and ^{18}F-dopa uptake: difference in Parkinson's disease and atypical parkinsonism. *J Neurol Neurosurg Psychiatry.* 1991;54:898–904.
28 Niimi T, Gotoh F, Ebihara S, et al. The effect of levodopa on cerebral circulation and metabolism in parkinsonism. *Acta Neurol Scand.* 1979;60(suppl 72):158–159.

29. Alexander GE, Crutcher MD, DeLong MR. Basal ganglia-thalamocortical circuits: parallel substrates for motor, oculomotor, prefrontal and limbic functions. *Prog Brain Res.* 1990;85:119–146.
30. Alexander GE, Crutcher MD. Functional architecture of basal ganglia circuits: neural substrates of parallel processing. *Trends Neurosci.* 1990;13:266–271.
31. Narabayashi H, Okuma T. Procaine oil blocking of the globus pallidus for the treatment of rigidity and tremor of parkinsonism. *Proc Japan Acad.* 1953;29:134–137.
32. Dogali M, Fazzini E, Kolodny E, et al. Sterotactic ventral pallidotomy for Parkinson's disease. *Neurology.* 1995;45:753–761.
33. Wester K, Hauglie-Hanssen E. Stereotactic thalamotomy: experiences from the levodopa era. *J Neurol Neurosurg Psychiatry.* 1990;53:427–430.
34. Yoshida M, Fujimoto K. *Motor Disturbances.* New York, NY: Academic Press; 1987:111–118. *Neuronal Activities of the Basal Ganglia in Normal as Well as in Parkinsonian Animals*;. vol 1.
35. Kim HJ, Im JH, Yang SO, et al. Imaging and quantitation of dopamine transporters with iodine-123-IPT in normal and Parkinson's disease subjects. *J Nucl Med.* 1997;38:1703–1711.
36. Ichise M, Ballinger JR. SPECT imaging of dopamine receptors. *J Nucl Med.* 1996;37:1591–1595.
37. Schwarz J, Tatsch K, Arnold G, et al. ^{123}I-iodobenzamide-SPECT predicts dopaminergic responsiveness in patients with de novo parkinsonism. *Neurology.* 1992;42:556–561.